International Journal of the Physical Sciences Vol. 6(16), pp. 3851-3866, 18 August, 2011
Available online at http://www.academicjournals.org/IJPS
DOI: 10.5897/IJPS10.480
ISSN 1992 - 1950 ©2011 Academic Journals

Full Length Research Paper

A distributed transmission line model of cloud-to-ground lightning return stroke: Model verification, return stroke velocity, unmeasured currents and radiated fields

P. R. P. Hoole[1]* and S. R. H. Hoole[2]

[1]School of Engineering Taylor's University Malaysia.
[2]Office of Engineering, University of Jaffna, Sri Lanka.

Accepted 02 March, 2011

Among the various models for lightning return strokes (LRS) that exist, the lossy distributed transmission line (DLCR) model, it is shown herein, is a dependable, comprehensive and accurate model. The model contains inductance (L), capacitance (C), and the heat-loss resistance (R). Recently, many alternative models have been proposed, and the adequacy of the DLCR model (DLCRM) has been questioned because of some shortcomings in the previously reported DLCRM simulation results. This paper corrects some of these shortcomings, such as correct representation and computation of the LRS current pulse wavefront, and the special nature of the attachment point at the earth end. In this paper where the DLCRM model proposed is a self-consistent model, within the assumptions stated and justified, it is shown that the LRS velocity predicted by the DLCRM is about fifty to seventy percent less than the velocity of light (for example, c/3). The velocity determined from the DLCRM presented here agrees with the measured LRS velocity, and captures also the drop in velocity as the LRS moves away from the segments away from the ground. When considering both the physical principles and observations of the earth flash lightning return stroke (LRS), the DLCRM yields results that are consistent with lightning measurements. The DLCRM may be used to obtain important engineering parameters which are not easily measured; one such example is the very high rate of rise of currents on a submicrosecond timescale (for example, 98 kA/μs), whereas the microsecond rate of rise of current may be a tenth of the submicrosecond values. Relating the computed electric and magnetic fields radiated by the LRS currents obtained from the DLCRM shows the correlation between the LRS current waveforms and the electromagnetic field waveforms at different distances from the LRS channel. Moreover, for unbranched first and subsequent return strokes, the model's electrical parameters such as inductance (L), capacitance (C) and resistance (R) values may be calculated from basic principles, with the assumptions made clearly defined and justified. Among the various models for lightning return strokes, the lossy transmission line model (the DLCRM) remains the most dependable when considering both the physical principles and measurements that provide a consistent and self-contained justification for the LCR model.

Key words: Lightning return stroke, transmission line model, lightning rate of rise of current, lightning radiated electromagnetic fields.

INTRODUCTION

Although the frequent lightning flashes are the flashes that occur within a thunder cloud (intra-cloud flashes) the most frequently studied flashes are those which occur between the thunder cloud and ground. These earth flashes are of most interest from an engineering point of view because of their close interaction with power and telecommunication systems, aircraft and rockets in flight close to a thunderstorm, and the threat they pose to

*Corresponding author. E-mail: prphoole@gmail.com.

various electronic systems, and to human life in a limited sense. A single lightning flash between a thunder cloud and earth may last for half a second. This single flash will contain the first return stroke and two to three subsequent return strokes. Each of these strokes may last for about one hundred milliseconds, with an interval between each stroke. Each stroke is made up of a rapidly moving current pulse (electromagnetic pulse) with submicro-second rise times and fractional changes. Even when the cloud to ground flash does not directly attach itself to an electronic system or electrically sensitive object (for example, a rocket), it radiates electromagnetic waves with submicrosecond changes which may interact destructively with avionics and ground electronic systems.

The mathematical modelling and computer simulation of the earth to ground flashes are not only of interest from the perspective of gaining greater knowledge of lightning physics (since it yields parameters which are normally not measurable, such as currents through the channel above the ground), but lightning return stroke simulations may help us also to predict and take protective action of lightning's (that is, earth to ground flash) effects on airborne and ground vehicles and systems. This paper is organized as follows: First, general measured characteristics of lightning return stroke currents and radiated electromagnetic fields will be discussed. Secondly, the origin of the electrical circuit model of the lightning return stroke, the lumped circuit model, is presented. Thirdly, the transmission line model and the dispersion characteristics, that is the quasi-transverse electromagnetic (quasi-TEM) wave and the distributed circuit model, are considered. Fourthly, the accuracy of the numerical solution of the quasi-TEM return stroke wave is tested. Fifthly, simulation results of the downward earth flash return stroke, including, currents and voltages are presented.

Lastly, an analysis of the LRS currents and the radiated electromagnetic pulses (LEMP), calculated from the DLCRM currents are compared to measured LRS currents and LEMPs.

ANALYSIS OF EXPERIMENTAL DATA OF LIGHTNING RETURN STROKE

Background

Photography, current measurements, and electromagnetic field measurements have been extensively used since the early days of lightning research. Boy's camera in 1926 originated the era of lightning photography (Schonland, 1956). The progressions of both the lightning leader and the return stroke have been photographed. These photographs first showed the stepped nature of the first leader, and gave good estimates of the bright tips observed in the stepped leader, the dart leader and the return strokes well above the ground. Photography has also been extensively used in triggered lightning investigation (Feiux et al., 1978; Rakov et al., 2005) to obtain the geometry of the return stroke channel, and the stroke velocities. Return stroke currents have been measured (Berger et al., 1975; Berger, 1977) by measuring the current along a tall conductor struck by lightning. These measurements gave an idea of the return stroke peak current, current rise rate, the action integral and the current wave forms at the foot of the channel.

Electric field changes due to the leader (L –change), return stroke (R – change) and continuing discharge (C – change) have been recorded (Lin et al., 1979; Weidman and Krider, 1980; Orville and Idone, 1982; Uman, 1985; Rachidi et al., 2001; Masaddeghi et al., 2007). These records further reveal short, sharp pulses during intervals between component strokes (J – change) as well as during the flow of continuing currents (M- change). Recent electromagnetic field measurements have sought to measure sub-microsecond changes and fields from positive flashes. Spectroscopic measurements (Shumpert et al., 1982) and sound measurements too have been made (Few, 1981; Ajayi, 1972; Balachandran, 1983). There are not many spectroscopic measurements available, and what has been analyzed does not agree well: there are obvious practical difficulties in getting a clean light spectrum of lightning. A lack of correlated measurements does make the understanding of data precarious. Although artificially (rocket) triggered lightning lends itself to correlated measurements, there is still much work to be done to correlate and interpret them in agreement with the physics of lightning. Moreover, the relation between natural lightning and artificially triggered lightning is another area in which more precise work still needs to be done.

A review of the important measurements that are pertinent to natural lightning return stroke modelling is given as follows with comments. A most exhaustive amount of data has been obtained for return stroke currents, return stroke velocity and the lightning electromagnetic pulse (LEMP).

Lightning current and electromagnetic field measurements

Although the lightning phenomenon has been observed for centuries (mainly associated with light and fire) it is only in the past sixty years that a massive amount of data has been published on the lightning discharge, the major part of it being confined to earth (cloud - to - ground) flashes. The most notable work has come from Schonland (1930's to 1950's), Berger (1960's) and Uman and associates at the University of Florida (1970's to date). Schonland's work (Schonland, 1956; Schonland et al., 1935) forms a good foundation. Berger's work (Berger

Table 1. Characteristics of return strokes, negative flashes, positive downward strokes and upward strokes flashes.

	First strokes	Subsequent strokes	First strokes	Subsequent strokes	Stroke first
Peak current (kA)	30	12	07	08	4.6 to 250
Maximum current di/dt steepness (kA/μs)	12	40	5	13	0.2 to 32
Time to crest (μs)	5.5	1.1	4	1.3	3.5 to 200
Time to half value (ms)	75	32	35	31	25 to 2000
Impulse charge (C)	4.5	0.95	0.5	0.6	2 to 150
$\int I^2 dt$ (A^2 s)					-1.5×10^7
Total charge (C)	5.2	1.4	__	__	__
Flash charge (C)	7.5	__	__	__	80
Av. velocity (m/s)	0.7×10^8	0.8×10^8	__	__	__

Note: A flash is defined as a sum of individual strokes (that is, a sum of the first and all subsequent strokes).

Table 2. Significant electric field measurements reported for downward negative flashes by different authors for maximum rate of rise of typical vertical electrical fields rise times at 100 km (kV/m/μs) (μs).

	First strokes	Subsequent strokes	
(Tiller et al., 1976).	3.	2.5	3.0.
(Lin et al. 1973, 1979)	2.15, 1.7, 2.8 and 1.2.	2.3, 1.56, 3.3 and 1.08.	2.0.
(Cooray and Lundquist, 1982; Cooray, 1984)	0.76.	---	7.0.
(Uman, 1985; Fisher and Uman, 1972).	1.4.	1.4.	4. ,1*
(Weidman and Krider, 1980, 1982).	45.4.	20 and 40.6.	0.1*

*10 to 90% rise times.

et al., 1975; Berger, 1977; Berger, 1967) is the best and most comprehensive. Uman's output (Uman, 1969; Rakov and Uman, 2003) is massive, spanning over 40 years, though still inconclusive and at times controversial in its interpretation with regard to the empirical return stroke models developed on the basis of the observed electric and magnetic fields. There is indeed a great need for different schools of thought on lightning to come together to work towards an understanding and mathematical modelling that is not only consistent with the measurement but also with the plasma and electromagnetic principles that underlie the observations. A summary of measured parameters of earth flash return stroke is given in Tables 1 and 2. From Table 1, it is obvious why the positive strokes, mostly observed in winter thunder storms, are more severe. The peak current of a positive first stroke can be as high as 250 kA, whereas for a negative stroke it is around 30 kA. However, if we consider that the destructive power of the lightning current is to be associated with the rate of rise of current, the negative stroke is more severe because of the lower rise times when compared to the positive flashes.

The energy associated with the flash is the action integral, and the return stroke velocity (which determines the return stroke current) is seen to be about three to four times less than the velocity of light. Some of the values that characterize lightning radiated electromagnetic fields or pulses (LEMPs) are given in Table 2 with some reservation. References are included to show some of the differences in observed data given by various workers. Some of the differences may be due to greater accuracy of the observation equipment used in some cases. This is the case for the high value of 45.4 kV/m/μs for the first LRS and 40.6 kV/m/μs (subsequent LRS) observed for maximum rate of rise of electric field (Weidman and Krider, 1980). The difference is due to the sub-microsecond rise times that the measuring equipment was able to capture (Weidman and Krider, 1982). Measurements made in the USA (Lin et al., 1979; Uman, 1985), and Sweden (Cooray and Lundquist, 1982) may show discrepancies due to the differences in the terrain over which the LEMP travels before being captured by the measuring equipment. Moreover, the values shown in Table 2 are for fields measured at close distances to the flash and then normalized to 100 km by a 1/D factor, where D is the distance from the flash.

The strokes sampled in Sweden number about five hundred (flashes), the other figures are from a sample of around 100 flashes (Lin and Uman, 1973; Cooray, 1984). The standard deviation for the first strokes is higher, and the values thus have a wider spread; this could be a

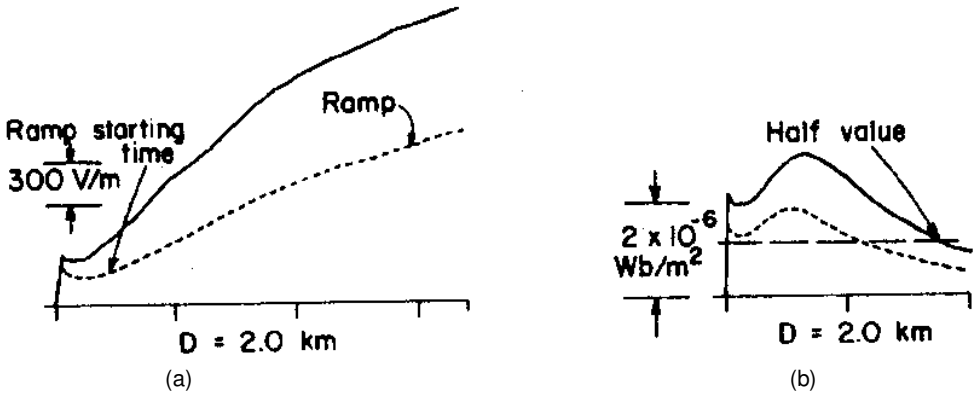

Figure 1. Measured (a) electric (in V/m) and (b) Magnetic field (in Wbs/m^2) at 2 km away from a first (solid line) and subsequent (dotted line) return strokes. Taken from (Uman and Krider, 1982) as adapted from (Lin et al., 1979). The measured fields shown are from 0 to 100 μs.

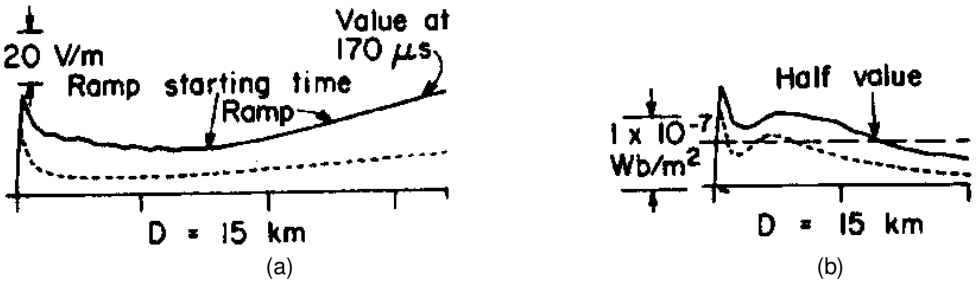

Figure 2. Measured (a) Electric (in V/m) and (b) Magnetic field (in Wb/m^2) at 15 km away from a first (solid line) and subsequent (dotted line) return strokes. Taken from (Uman and Krider, 1982), as adapted from (Lin et al., 1977). The measured fields shown are from 0 to 100 μs.

possible reason for the discrepancy in the ((dE/dt) first LRS/(dE/dt) subsequent LRS) ratio reported by different workers. The higher dE/dt values observed (Weidman and Krider, 1980) are due to the 10 to 90% rise times of around 100 ns which were observed, in comparison to the 1 μs observed by others. Another interesting feature is that the first stroke fields have a lower rate of rise than the subsequent strokes. In Figures 1 and 2 are given the measured electric and magnetic fields at a distance of 2 and 15 km away from the lightning flash (Lin et al., 1979; Uman and Krider, 1982). Note that in both cases there are common features in the electric field at 2 and 15 km: an initial peak, then a dip, and finally a closely increasing ramp like tail. Similarly for the magnetic field: an initial peak, followed by a dip, and then a hump which slowly decays. When we model and implement an LRS model, we will expect the electric and magnetic fields calculated from the LRS currents obtained by the LRS model to resemble the measured electric and magnetic fields. In order for LRS simulation algorithms to be able to capture such significant values, it should be able to estimate submicrosecond changes in the LRS current wavefront correctly.

From the LRS currents calculated by an LRS simulation model, it is important to be able to estimate large values of rate of rise of electric fields correctly, since it is this quantity that poses a great threat to aviation electronics, and induces surges on electric power transmission and distribution systems even when there is no direct strike to the object. The DLCRM reviewed in this paper is able to do this, without any artificial alterations in the L, C or R values or make mathematical adjustments in the model. Some parameters are calculated from observations made. For instance, the return stroke velocity is calculated from the time for the luminosity of the LRS to peak at discrete points as the LRS current pulse speeds along the channel towards the cloud (Jordon and Uman, 1983; Idone and Orville, 1985). In our consideration of LEMP calculations we shall also look at the interpretation of measured LEMP.

THE EMPIRICAL MODELS: LUMPED CIRCUIT MODEL AND THE CURVE FITTING MODEL

There are, in general, two different approaches to LRS modelling which continue to be developed and discussed.

These are what we may term as the “empirical models” and the distributed inductance-capacitance-resistance transmission line model (DLCRM). There is a third category, which is the shock wave model (SWM), where gas dynamics theory is applied to the presence of high pressures along the lightning channel axis, associated with the lightning leader tip, the return stroke wavefront and the subsequent radial shock wave that results in thunder, an acoustic wave (Fowler, 1982; Braginskii, 1958). For instance, the LRS is considered as a non-linear electron acoustic wave (Fowler, 1982).

It has received less attention since it has been found inadequate to explain or properly represent the important electrical characteristics observed in LRS, and using the model requires detailed knowledge of thermal and electrical conductivities, recombination and ionization coefficients, as well as simultaneous solutions of Maxwell’s equations, and momentum, energy and mass equations (Spitzer, 1961). Moreover a convincing case can be made to show that the LRS is a quasi- transverse electromagnetic wave (quasi-TEM) moving along an un-magnetized, ionized, plasma channel, which in turn allows the lightning channel to be modelled by a lossy transmission line along which energy flow is sustained by a quasi-TEM wave (Hoole and Hoole, 1988).

The lumped circuit model (LCM)

The origin of the LCM, also called the Bruce-Golde model (Bruce and Golde, 1941), may be traced back to the fact that the lightning return stroke currents measured at ground level, very much resemble the time domain waveform of voltages in the long high voltage sparks produced in the high voltage laboratories used for testing power system equipment for lightning surges (Bruce and Golde, 1941). We may best illustrate this model by using simple circuit theory. Very crude, intuitive models for the leader and the return stroke are a capacitor(C)-resistor(R) circuit to which a stepped voltage V(t) is applied and a charged capacitor (C)- series inductor(L)-resistor (R) circuit (part in red is an incomplete sentence). In the case of the leader, as the stepped leader progresses downward, for each leader step, a step voltage V(t) from the thundercloud is applied to the series CR elements at the cloud end. The leader channel is represented by a resistor R, and the electrostatic energy stored at the tip of the leader is represented by a capacitor C between the leader tip and the ground. Thus the nature of the leader is here represented by an RC circuit triggered by a constant voltage source, which produces a leader current I(t), for which we get:

$$RI(t) + 1/C \int I(t)\,dt = V(t) \qquad (1)$$

On differentiating Equation 1 and solving the resulting differential equation:

$$I(t) = \exp(-t/RC) \int (1/R) \exp(t/RC)\, dV/dt + Io \qquad (2)$$

where I_o is the continuing current flowing along the lightning leader channel.

After the initial rise of V, the voltage that drives the leader current, if we should consider dV/dt = 0, the leader current is simply Io exp (-t/RC) and is sketched in Figure 1b. At each step, the leader will be visible as a bright light pulse, which rapidly decays in intensity, following the current which produces the visible light radiation (Idone and Orville, 1985). If we assume significant magnetic energy in the leader, then the leader current characteristics will also look like the LRS lumped circuit current characteristics. In the case of the return stroke, assume that all the cloud charge is transferred to the leader as the leader is connected to the ground. Thus representing the charge stored in the leader by a capacitor C (Bruce and Golde, 1941), and the lightning leader channel being considered as a resistor (R) and inductor (L) in series, then the return stroke current flows when the leader channel becomes attached to the ground. For the lumped LCR circuit, Kirchhoff’s law gives:

$$LdI/dt + RI + 1/C \int Idt = 0 \qquad (3)$$

Differentiating (3) gives:

$$L\, d^2I/dt^2 + R\, dI/dt + I/C = 0 \qquad (4)$$

This has the solution form:

$$I(t) = A \exp^{(1)}\left[\frac{-R-K}{2L}\right]t + B \exp\left[\frac{-R+K}{2L}\right]t \qquad (5)$$

where,

$$K = (R^2 - (4L/C))^{1/2} \qquad (6)$$

Using I(t) = 0 when t = 0 we obtain:

$$I(t) = I_m\left[\exp\left[-\frac{R-K}{2L}t\right] - \exp\left[-\frac{R+K}{2L}t\right]\right] \qquad (7)$$

where I_m is the peak LRS current. The form of (7) resembles the Bruce-Golde model and is sketched in Figure 2b. Differentiating (7) and setting dI/dt = 0, we have the rise time given by:

$$t_T = \frac{L}{K} \log_n\left[\frac{R+K}{R-K}\right] \text{ seconds} \qquad (8)$$

which is a strong function of L/R, when $R^2 >> 4L/C$ and K ~ R. We note that the important parameter t_T depends on careful estimation of L/R. We shall note later that in (Little, 1978) for the current at the earth end, and in

Strawe (1979) as well L/R at the earth end has been set to zero or close to zero. Thus the distribution LCR models of Little (1978) and Strawe (1979) are unreliable for rise time estimation. In computation it is important to keep the time step $\Delta t << L/R$, and the accuracy is easily checked by ensuring there are computed points on the wave-front.

The curve fitting model (CFM)

The lumped circuit model (LCM) does not simulate the travelling wave scenario of the LRS. In order to overcome this fundamental weakness in LCM, several papers have been published to specify the current-time and current–height characteristics of the LRS as it travels along the leader channel (Lin et al., 1979; Master et al., 1981; Deidendorfer and Uman, 1990; Rakov and Uman, 1998; Moosavi et al., 2009; Baba and Rakov, 2005; Cooray, 2003; Baba and Rakov, 2007). The curve fitting nature of these empirical models goes one important step beyond the LCM. Whereas the LCM was concerned solely about a waveform that matches the lightning currents measured at ground level, the CFM models searched for a model that will also yield radiated electromagnetic fields that have been measured (Idone and Oriville, 1985). The LRS current waveforms are made up of three different current components, of which one is a direct current component, and another is the Bruce-Golde like double exponential current (Bruce and Golde, 1941). Parameters such as the peak current, the time constants, and the velocity of the return stroke may be obtained from ground measure-ments, including those of currents and/or the lightning radiated electromagnetic pulse LEMP (Uman and Standler, 1980).

The empirically specified parameters of current-time characteristics are adjusted to get the measured radiated fields radiated by the LRS currents along the channel. Some of the more recent LCM and related models which spill over into modifications of the DLCR models (further complicating, blurring, the issues at times), sought to specify conductivity-time characteristics, or LRS radius-time characteristics in order to get time varying electric field and magnetic field signatures that closely resemble measured electric and magnetic fields (Master et al., 1981; Deidendorfer and Uman, 1990; Moosavi et al., 2009; Baba and Rakov, 2005). It is a curve fitting method, without a well reasoned out or self-consistent LRS model: keep changing the current waveforms, calculate the radiated electromagnetic fields from it, and then get back to adjust the current waveforms and numbers such as peak current, rise time, attenuation along the channel or direct current, until the calculated radiation (electric and magnetic) fields match the measured radiated fields. However, it is open to question whether such models are true to the LRS physical processes and whether they may rightly be called engineering models (Hoole and Hoole, 1988, 1996) of the LRS. We hope that in the future, all those that are at the cutting edge of lightning research will come to a consensus on terms and definitions.

The CFM models have been further extended by exploring the effects of an assumed corona layer surrounding the lightning channel (da Mattos and Christopoulos, 1988, 1990), or by assuming a two component electric charge density flow, with different time constants to get radiated electric fields closer to the measured electric fields (Thottappillil and Uman, 1994; Tiller et al., 1976).

THE DISTRIBUTED CIRCUIT, TRANSMISSION LINE MODEL (DLCRM)

Background to the DLCRM

The second approach is to model the return stroke by the LCR transmission line, DLCRM (Little, 1978; Strawe, 1979; Moosavi et al., 2009; Price and Pierce, 1977; Theethayi and Cooray, 2005; Cooray and Theethayi, 2008; Hoole, 1993; Hoole and Hoole, 1993). For the model to have self -consistency, it has been shown that it is proper to represent the LRS by a quasi-TEM wave travelling along a lossy transmission line. The L, C and R elements of the line may be determined from basic electromagnetic principles (Hoole, 1993). In the original work done on DLCRM (Little, 1978; Strawe, 1979; Price and Pierce, 1977).the case was made that the DLCRM is attractive for the determination of currents even above ground level, which could also include the presence of an aircraft, lightning conductor or transmission tower. The short comings of the earlier work, sometimes unknowingly carried on in more recent work, may be worth pointing out so that extra care is taken when developing and coding the DLCRM:

1. The distributed transmission line solution should allow the length of each segment explicitly to play a role in the numerical calculations. The L, C and R values must remain per unit length values, and the length of the segment must not be multiplied into the L, C and R values to become lumped elements. During numerical computation, the length of each segment and the time step used are correlated to ensure that during each iteration, the current wave must not travel into the next element. If lumped element segments are used as in (Little, 1978), the lumped elements add to the numerical error and limit the values of the elements and their layout because of stability problems.
2. In computing the current in the first segment (stemming from the attachment point to the ground) by considering it as a CR element (Little, 1978), or allowing the resistance to be very large (Strawe, 1979) so as to allow it to suppress the effect of inductance L, a singularity point is created and the current will be expected to go to infinity. In (Strawe, 1979) the L/R ratio

is about $0.1X10^{-6}$ s, if the 16 ohms/m resistance value is used, leading to the same situation as found in Little (1978) for the attachment segment. This is one reason that a proper wavefront was not obtained for the ground level LRS current. The wavefront is drawn by the computer as a straight line jump from zero to the peak current. It is always a good practice to ensure that points along the wave front are calculated (Hoole and Hoole, 1993).

3. The connecting leader must not be assumed to be only made up of a resistance element. The upward leader, with the increase in current flowing in it just before connection with the downward leader from the cloud, it would be carrying a significant amount of current. Hence the energy in the connecting leader magnetic field cannot be ignored, and an L element must be assigned to it as well as the downward leader. Just before the return stroke is initiated, the downward leader transforms the connecting leader into an arc channel which is able to carry the large return stroke current.

4. It is not necessary to resort to the complex finite difference method (FDM) of computation of electrostatic fields to obtain the distributed capacitance of the lightning channel. The problem involved herein is the arrangement of the electrode system with the cloud charge and the leader charge. An unrealistic cloud structure such as a 100 m sphere or a 15 km long plane electrode was used to obtain reasonable values for the capacitance (Little, 1978). In order to do an FDM computation the potential at a height of 15 km is set at 15 MV for a 100 m cloud charge at 100 MV. Instead of such unreasonable assumptions being made, it may be shown that a simple charge simulation computation for the leader channel vertically above a perfectly conducting earth, gives reasonable values for the channel (Hoole, 1993). It was also observed that the capacitance close to the earth end will be larger since there is more stored energy expected between the sharp edge of the leader and the ground. This produces the large LRS current at the earth end, and a lower return stroke velocity at the lower end of the lightning channel.

5. Following the earlier DLRCM using time varying resistance (Strawe, 1979), recent models have also resorted to DLCRM (Moosavi et al., 2009). Braginskii's model Braginskii (1958) for a spark channel is used to obtain a time varying radius r (proportional to $t^{1/2}$) (Strawe, 1979). A curve fit to the work is used to obtain a time varying conductivity (Plooster, 1971; Strawe, 1979). A clear discussion of the use of theories other than Maxwell's equations needs more extensive discussion (Uman, 1987). But what is important to point out is that the claim that time varying resistances, and time varying spatially varying inductances are necessary to obtain calculated electric and magnetic fields resembling measured fields (Moosavi et al., 2009; Theethayi and Cooray, 2005) are incorrect. Using Maxwell's equations for static electric fields and static magnetic fields, capacitance and inductance values may be obtained to yield LRS currents that yield convex wavefront current at ground level, as well as radiated electric and magnetic fields that match the measured fields (Hoole, 1993; Hoole and Hoole, 1993).

6. The trend to put more and more details into a model must be carefully justified. When such details are put in, it is also important to keep a close check that the computer is giving results that may be checked out, and compared with analytical solutions, such as for the diffusion equation (Hoole, 1993) and for different numbers of transmission line segments (for example, 10 and 30) for the same simulation problem. Time steps must be carefully chosen (LCM). What is sometimes called the electromagnetic models of LRS (Moosavi, 2009), are mere variations of the DLCRM, and may be tested out using the same kind of verification simulations. When the Finite Difference Method is used with time stepping (Baba and Rakov, 2007; Rakov and Uman, 1998), it is important to ensure that time steps are properly coordinated with the size of the grid, and that the different velocities of the wave along the lightning channel (for example c/3, where c is the velocity of light) and the velocity of the wave being radiated out into space (which is equal to c) are properly accounted for.

The transmission line dispersion relation

Using electromagnetic theory, that the values for L and C determined for the lightning channel are not very different to a crude coaxial system may be seen by considering a 1 cm lightning channel to be surrounded by an outer cylinder of cloud radius (for example 1 km) (Hoole, 1993). The inductance and capacitance are 2 µH/m and 5.5 pF/m respectively. The capacitance very near the earth is large since the energy stored there will be large. The velocity of the return stroke measured well above the earth (for example 200 m), shows a wave velocity of about 0.3c where c is the velocity of light. However at such heights well above ground the computed LRS channel inductance and capacitance values yield $1/\sqrt{LC}$ of the order of c, the velocity of light. This is the case for overhead power and telecommunications lines. Since measured electromagnetic fields appear to show that the bulk of the energy is transmitted by a group of waves centred around 5 kHz (Uman, 1987), we examine here the dispersion curve for a linear transmission line with L,C and R values close to what has been calculated. For the approximate equivalent circuit of a short length of line with:

R = Series resistance per unit length of line.
L = Series inductance per unit length of line.
C = Shunt capacitance per unit length
G = Shunt inductance per unit length,

it can be shown that the attenuation constant of the

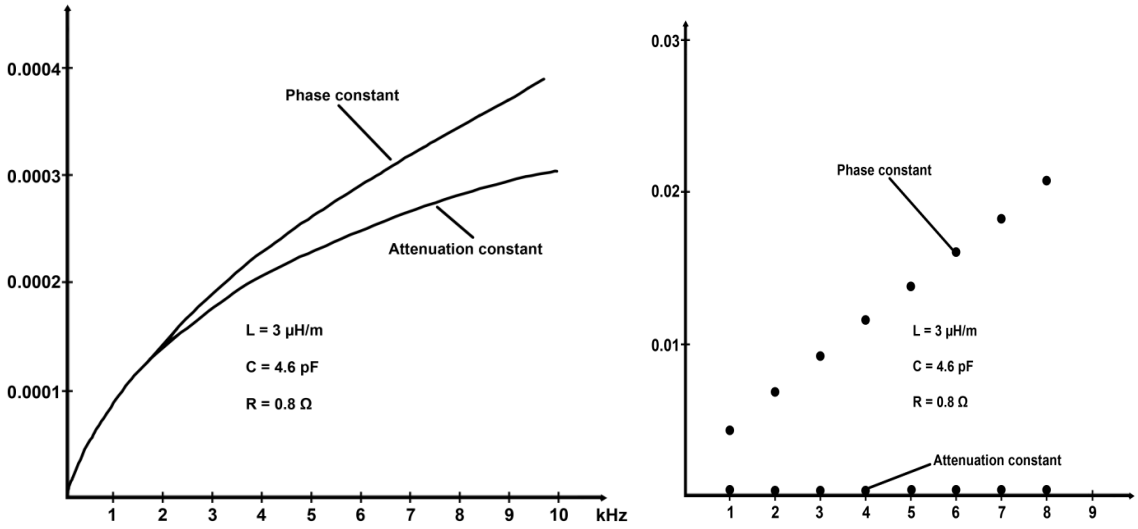

Figure 3. The Dispersion Characteristics of a distributed LCR Line. The attenuation constant α is in nepers/m and the phase constant β in radians/m. Adapted from (Hoole and Hoole, 1988).

quasi-TEM wave along the transmission line is (Hoole, 1993):

$$\alpha = \frac{1}{\sqrt{2}}\left[(RG - \omega^2 LC) + \{(R^2 + \omega^2 L^2)(G^2 + \omega^2 C^2)\}^{1/2}\right]^{1/2} \text{ nepers/m} \quad (9)$$

The phase constant is given by:

$$\beta = \frac{1}{\sqrt{2}}\left[-(RG - \omega^2 LC) + \{(R^2 + \omega^2 L^2)(G^2 + \omega^2 C^2)\}^{1/2}\right]^{1/2} \quad \text{radians/m} \quad (10)$$

The wave propagates along the line at a velocity $V_p = \omega/\beta$, known as the phase velocity with the amplitude decaying with distance as exp (-αz). If a group of waves whose frequencies lie between ω and ω + dω is considered, the resultant amplitude envelope of the group, which carries the energy contained in the signals, travels down the line at a group velocity $V_g = d\omega/d\beta$, assuming the β – ω curve to be a straight line between ω and ω+dω. For G = 0, the β-ω and α–ω plots are given in Figure 3. As expected, for ωL>>R, that is at very high frequencies, $\omega/\beta = 1/\sqrt{LC}$, the wave is travelling at the velocity of light. This is the region where the β – ω plot becomes a straight line. At low frequencies, with ωL<<R, we have $\beta = \sqrt{\omega}\sqrt{RC}/\sqrt{2}$; that is α and β vary as √ω, which is parabolic in shape.

The condition where the resistance is negligible is only reached in the frequencies above 1 MHz for channel resistance R = 0.8 ohm/m at about 10 MHz for R = 5 ohms/m. Therefore in the frequency ranges of interest in LRS the phase and group velocities will be less than the velocity of light. Although we do not deal here with very high frequency signals, it is interesting to note that α from (9) goes through a peak and at very high frequencies approaches $1/\sqrt{2}(R^2C/L)$.

Numerical solution of the transmission line wave equation

The finite difference solution of the wave equation

For conductance G = 0 and a wave travelling along the z-axis, the basic equation we seek to solve numerically is (Hoole and Hoole, 1996):

$$\frac{\partial^2 V}{\partial z^2} - RC\frac{\partial V}{\partial t} - LC\frac{\partial^2 V}{\partial t^2} = 0 \quad (11)$$

Having solved for V, the current may be obtained by integrating the equation:

$$I = -C\frac{\partial V}{\partial t}dt \quad (12)$$

We retain the partial differential equations since we are interested in the distributed-parameter field phenomena. We may now recast (11) using the finite difference approximation as (Hoole and Hoole, 1996):

$$\left(\frac{R\Delta t}{2} + L\right)V_n(z, t - \Delta t) + 2\left(L - \frac{\Delta t^2}{C\Delta z^2}\right)V_n(z, t) + \frac{\Delta t^2}{C\Delta z^2}\left(V_{n+1}(z + \Delta z, t) + V_{n-1}(z - \Delta z, t)\right) \quad (13)$$

and (12) by:

$$I_n(z, t) = I_0 + \sum_{i=1}^{n}\left(\frac{V_i(z,t+\Delta t) - V_i(z,t-\Delta t)}{2\Delta t}\right)C_i \quad (14)$$

where V_n and I_n are the voltage and current at the n-th segment of the transmission line.

The potential V along the leader is set equal to the cloud potential. This is a valid initial value, since the column field drops in an atmospheric air arc carrying 10 A is about 5 V/cm (von Engel, 1983). For a 3 km channel the total column potential drop will be 1.5 MV, ignored here compared to the 60 MV or more cloud potential. It is useful to note that for a leader current of 300 A, and a channel resistance of 2 ohms/m, the column field) is 6 V/cm (which gives rise to the potential drop of about 1.8 MV over a 3 km long channel, which is in good agreement with the laboratory arc value. For the perfectly conducting earth, the potential behind the earth resistance is set at zero. The Equations 13 and 14 could be readily solved by a time stepping process, where the time step is kept small compared to $\Delta z \sqrt{LC}$ and L/2R, in order to obtain a stable solution with sufficient number of calculated points appearing on the wavefront. The distance step Δz is chosen so as to keep it longer than $2\Delta t$. Whence to ensure a stable solution the following two steps are adopted (i) choose Δt such that it is small compared to L/2R. (ii) choose Δz such that it is greater than both $(\Delta t/\sqrt{LC})$ and $(2\Delta t)/RC$.

These conditions ensure stability of solution, whatever the magnitudes R, L and C are used in (13) and (14). This is roughly verified by considering the ratios $\Delta z : \Delta t/RC : \Delta t/LC$. Unless the user specifies a time step less than the minimum value of L/2R for each segment of the distributed LCR network, the routine automatically sets it to L/10R. It is therefore important to ensure that Δz is sufficiently large compared to $L\sqrt{C}/R$ and 2L/RC.

Testing the DLCRM computer code

a) Test 1: The accuracy of the LCR transmission line finite difference code was tested by comparing the calculations with the CR routine for the complementary error function. The current along the lightning channel, for a diffusion wave (Hoole, 1993) is given by:

$$\hat{\mathbf{i}}(z,t) = (V/R)\sqrt{(CR/\pi t)}\exp\left[1-\left(\sqrt{(CR/\pi t)}z^2\right)\right] \quad (15)$$

Setting the L, C and R values to obtain the diffusion wave, the numerical solution for currents using (13) and (14) were compared with those obtained from (14). A very good match was found (Hoole, 1993). This test was a double check on the reliability of the finite-difference, computer based solutions obtained from (13) and (14).

b) Test 2. A further test was done by using the coded DLCRM equations (12) and 13). For the same initial conditions, the LRS currents were computed for a ten segment lightning channel and a thirty segment lightning channel of the same length as for the ten segment line. Again very good agreement between the currents calculated at the same discrete points along the channel were observed (Hoole, 1993).

c) Test 3. The influence of time steps chosen on the current wavefront was also studied (Hoole and Hoole, 1993). For example, the wavefront was calculated with time steps 0.1 and 0.05 µs for a line with an L/R ratio of 0.55 µs. This test also revealed that a time step of 0.1 µs gives good convergence for the values of circuit parameters used in this paper to simulate the lightning return stroke.

Return stroke velocity and the transmission line model

Background

A fourth test of the DLCRM and the computer code developed is to observe the velocity of the LRS current pulse (a quasi-TEM wave) along the channel, and compare it to the measured LRS velocity. Obviously the return stroke currents determined from DLRCM are made of a wave train which is influenced in a complex manner by the return stroke channel, including reflections due to the finite length of the channel when currents are computed for a few tens of microseconds. Although we discuss phase velocities for signals of different wavelengths, the precise significance of phase velocity does not apply to the wave train of finite length generated at the earth end. For LRS currents it is the group velocity, and not the phase velocity that must be calculated from the current pulses, which must be compared with the measured lightning velocity. Since an electromagnetic field cannot completely be localized in either space or time, there must be an essential arbitrariness about every definition of velocity. For convenience, it is common to talk about the group velocity, phase velocity and the signal velocity (Hoole and Hoole, 1996).

The group velocity ($d\omega/dk$) is less than the phase velocity (ω/k) for normal dispersion (Lin et al., 1979), where $k (= 2\pi/\lambda)$ is the wave number and λ is the wave length.

Return stroke velocity: from photography and the DLCRM

Although the lossy transmission line model for quasi-transverse electromagnetic waves is an established tool, the question of velocity of the current wave train both that computed from the DLCRM (Background) and that measured, needs some discussion. We take the concentration of electromagnetic fields in space to indicate the energy to be localized in that region. Taking this to be the case, we plotted the times at which current peaks at different points on the line against the height for 1, 2 and 5 ohms/m resistances. The value of $1/\sqrt{(LC)}$ was set equal to 300 m/µs in order to be able to observe the influence of resistance; this setting is not unreasonable since the values for L and C calculated satisfy the

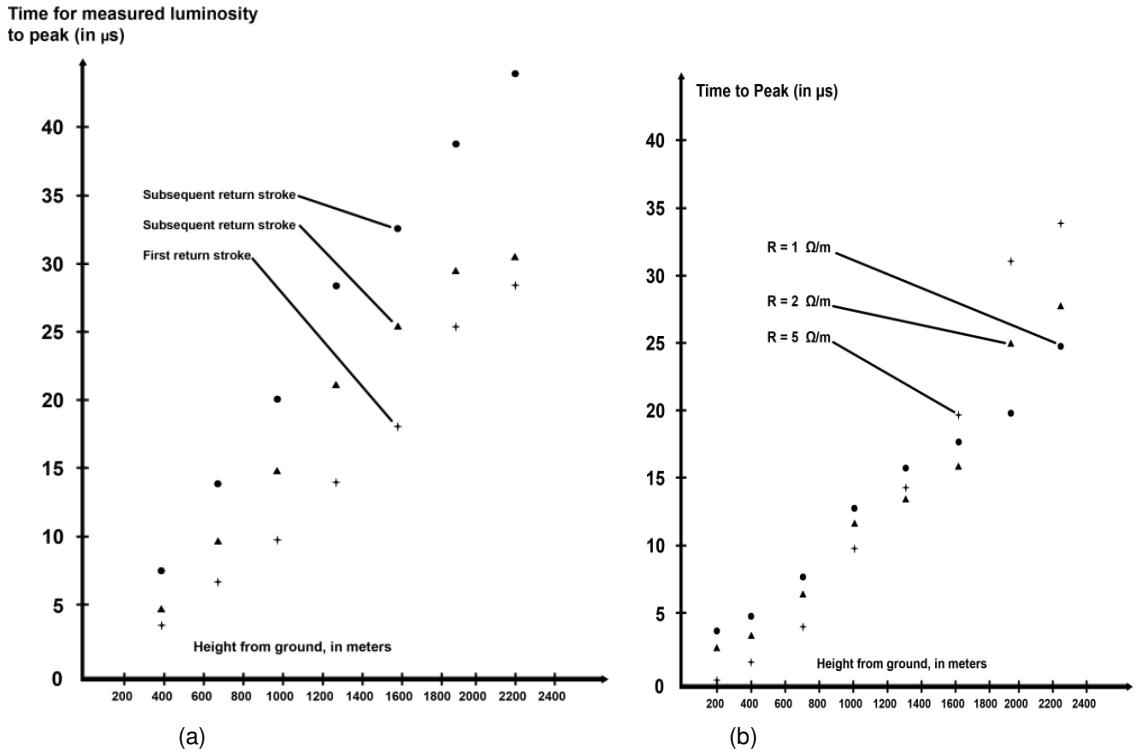

Figure 4. Times at which return stroke reaches peak value at different heights along the lightning channel (a) Calculated from DLCRM equations (13) and (14) for L = 2μH/m, C = 5.5pF/m and three values of R (5, 2 and 1ohms/m) (b) Measured LRS peak using photography of the luminous pulse moving up the lightning channel. Adapted from (Hoole and Hoole, 1988).

relationship $1/\sqrt{(LC)} = c$ away from the immediate vicinity of the ground (Hoole, 1993). The plots from DLCRM are shown in Figure 4a with measured values for three different LRS sets in Figure 4b, (Guo and Krider, 1982; Idone and Orville, 1985). The photographic measurements give times along the lightning channel when the return stroke luminosity is brightest (Jordon and Uman, 1983; Uman, 1987); and for the transmission line solutions, arrival times are the times at which DLCRM calculated return stroke current reaches peak values, as shown in Figure 4.

Both plots agree very well, showing a largely constant velocity along the channel, except for the LRS velocity close to ground. From the DLCRM calculated current waves, it was observed that close to the ground, the return stroke velocity is higher than the velocities calculated or measured above the ground. The average velocity in the case of the transmission line model, with all three cases of different resistance values taken together, is 73 m/μs (roughly c/4), where c is the velocity of light) agreeing well with 100 m/μs (c/3) average measured return stroke velocity. It should be noted that the DLCRM simulation results are not for exact lightning parameters for the LRS which Schonland photographed (Schonland, 1956); hence the differences (c/4 and c/3) are understandable and acceptable. A change of lightning channel resistance from 1 to 5 ohms/m results in a 26% increase in the group velocity. This change is within the 5% group velocity change for an LRS current wave packet with a centre of gravity at 100 kHz and the 50% change for a wave LRS current packet centered at 5 kHz.

The measured velocities are substantially less than the velocity of light c (= 3 x 10^8 m/s). Although the measured values for the LRS have been questioned (Idone and Oriville, 1985), the basis for the case against a LRS velocity less than c is questionable. In the LRS model used in (Cooray and Theethayi, 2008; Theethayi and Cooray, 2005), the L, C, and R parameters were calculated using assumptions that are not well supported. When the computer simulated LRS waves were seen to travel at an almost constant velocity close to the velocity of light (Idone and Oriville, 1985), it was stated that the error is due to the problems in luminosity measurements. On the contrary, in the DLCR model developed using electromagnetic field principles to determine the circuit parameters, especially L and C, it is seen that the DLCR model LRS current wave yields a velocity which is close to the measured LRS velocity (Hoole and Hoole, 1993). Moreover, for the case of 1 ohm/m channel, for instance, the LRS velocity changes were calculated from Figure 4a: 10^8 m/s (c/3) close to the ground; which then drops to

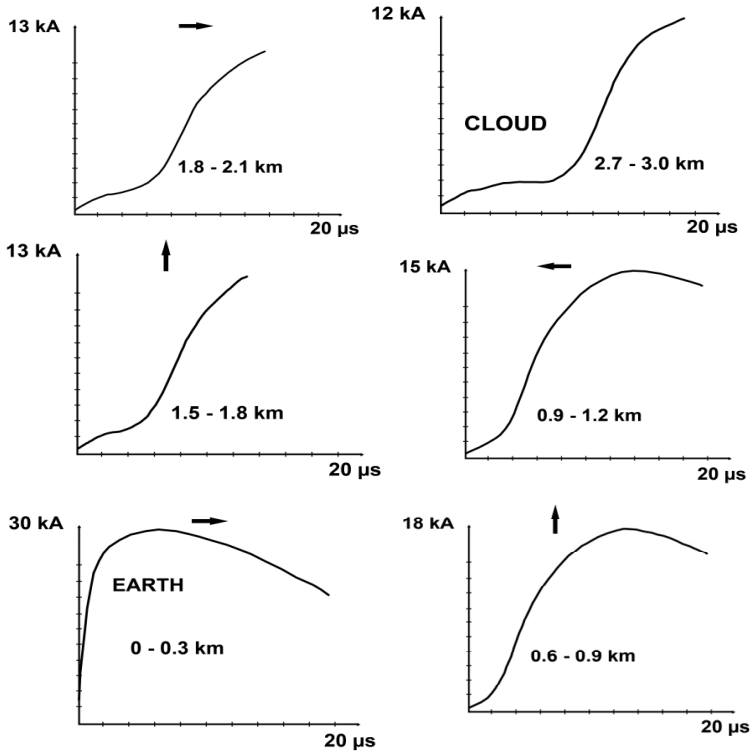

Figure 5. Current - height and- time characteristics for negative earth flash return stroke - Adapted from (Hoole and Hoole, 1993).

0.5 x 10^8 m/s (c/6) before settling down to a constant velocity of about 0.4 x 10^8 m/s all the way to the cloud.

For an increased value of the resistance, that is 5 ohms/m, the LRS velocity, from Figure 4, is reduced to about c/10 and is more constant and diffusion like over the length of the channel.

NEGATIVE CLOUD TO GROUND EARTH FLASH RETURN STROKE: SIMULATED BY THE DLCRM

Background

This is the most common type of flash observed. It appears over mountainous regions, as well as over sea. We shall consider the subsequent return strokes for the present. Two types of contact points are considered. In the first case, the flash is to an open ground, with a ground resistivity of 100 ohm-m, as in Florida. It is known that from fulgurites in sand, the radius of the contact point is about 0.03 to 0.52 cm, and that the flash does not progress into the ground for more than a metre. We ignore any movement of the stroke into the ground, since any melting into the earth will take place when the bulk of the charge will be lowered by the continuing current over a few tenths of milliseconds. Since the return stroke exists only for a few tens of microseconds, we take the contact point to be stationary and as a sphere with the radius of the channel. The earth resistance in this case might be in the range of 1 to 8 ohms. In the second case, where an earthed electrode provides the return stroke path to the earth, the earth resistance is in the range of 100 to 250 ohms for a conductor radius of 0.2 to 1 cm, buried 1 m in a soil of resistively 100 ohm-m.

The DLCRM simulation studies were carried out for the prescribed settings of the following parameters: radius of the cloud spherical electric charge centre (500 m), channel resistance R (0.8 ohm/m), inductance L (3 µ h/m), capacitance of the first segment at the earth end (25 picoF/m), capacitance along the segments other than the earth send segment (4.6 picoF/m), earth resistance R_E (1500 ohms), the length of the channel from ground to the base of the thundercloud charge centre (3000 m), the number of segments that the channel is divided into (10 segments, 300 m/segment), potential of the thundercloud electric charge centre (50 MV), the initial leader current along the channel (100 A), data obtained from (Berger et al., 1975; Berger, 1977, 1967).

LRS Currents from DLCRM simulation

The calculated currents and potentials of the LRS are given in Figures 5 and 6 (Hoole and Hoole, 1993). The electric field and magnetic field calculated using the currents yielded by the DLCRM simulation are given in

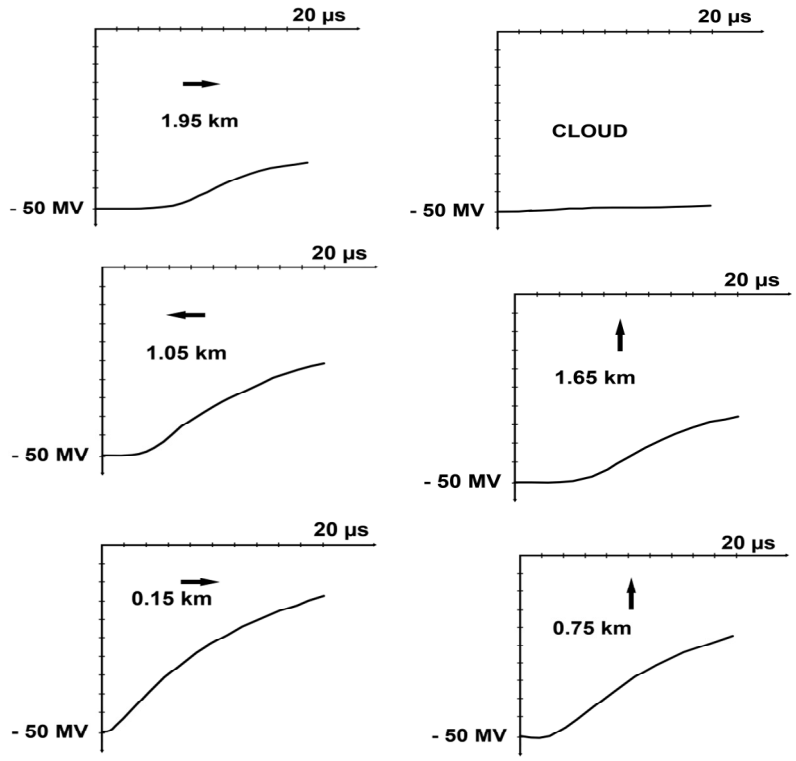

Figure 6. Voltage - height and- time characteristics for negative earth flash return stroke – adapted from (Hoole and Hoole, 1993).

Figures 7 and 8 respectively. The fields are calculated using the integral method reported in (Hoole and Hoole, 1987). From an engineering perspective we are primarily interested in the details of the waveforms over the first few tens of microseconds, when rapid, high current changes occur. Most of the calculations are carried out for the first 20 µs of the LRS. The current wavefront has two distinctive regions at the earth end. The DLCRM predicts the overall concave wavefront of the LRS current as seen in Figure 5. In the current waveforms we observe an initial slow rise of current, followed by a sudden rise to peak. Thus the overall current wave has a concave shaped wavefront. At heights above the earth, there are three regions in the current wavefront; a gradual variation in current, increasing to about 2 kA, before the main return stroke pulse arrives at a point along the lightning channel. Second, the LRS arrives at that point and a sharp rise of current is observed in the wave-front. Third, there is a slower increase towards peak current. From an engineering perspective the initial, slow ramp like increase of current is not the significant part of the LRS.

The portion after the ramp current, having a rapid rate of rise, is that which is severe with regard to the induced effects of lightning. This portion of the LRS current wavefront, that follows the ramp shaped current, is convex in shape. In a wonderful way, this DLCR model to which no additional currents, or curve fitting techniques using time changing radius or conductivity are added, gives an exact representation of the LRS current waveform. All these essential features of the LRS currents are carefully captured by the DLCRM. As expected, the wavefront degenerates with height, and the current crest decays with height (Uman and Krider, 1982; Baba and Rakov, 2005; Cooray, 1993). In general, it is observed that the luminosity of the return stroke does not significantly drop with height (Uman et al., 1982). The overall potential along the lightning channel drops as the LRS current pulse discharges the lightning channel segment over which it has traversed. Within the first 20 µs of the LRS, close to the ground the channel potential may drop from about 50 MV to about 15 MV and close to the cloud to about 40 MV (Figure 6). This is rapid discharge of electric charges. As the electric charges in the thundercloud are emptied into the ground through multiple leader-return stroke occurrences, the potential will drop as the thundercloud becomes discharged. If needed, the electric field inside the channel E_c may be determined from the potential profile in Figure 6, or from the current density $J = \sigma E_c$.

LRS electric and magnetic fields calculated from currents obtained from DLCRM simulation

The electric fields and magnetic fields radiated by the

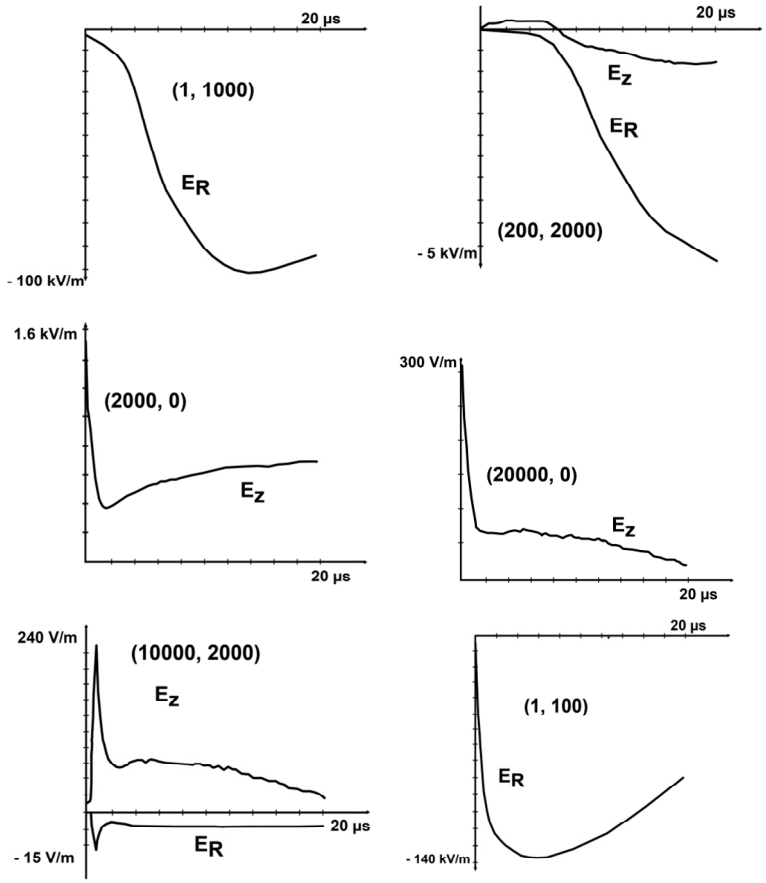

Figure 7. The vertical (E_z) and horizontal (E_R) electric fields radiated by the downward negative earth flash return stroke. The bracketed numbers in the form of coordinates (x,y) indicate the spatial point at which the fields were calculated – adapted from (Hoole and Hoole, 1993).

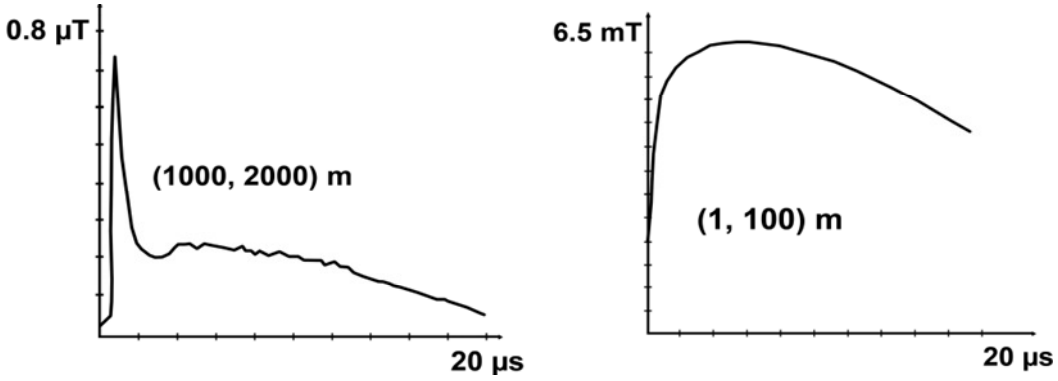

Figure 8. Magnetic fields radiated by the downward negative earth flash return stroke – adapted from (Hoole and Hoole, 1993).

current pulses are given in Figures 7 and 8 respectively. The fields are generally in good agreement with the ground measurements. The fields were calculated using the integral technique (Hoole and Hoole, 1987). It is important to note that the DLCRM gives a correct picture of the radiated electromagnetic pulse (LEMP) without any

artificial, forced features such as added ramps or time varying radius or time varying conductivity being added on to the model. Comparing the electric and magnetic fields calculated from the DLCRM LRS currents (Figures 7 and 8) to the measured fields (Figures 1 and 2), we note that there is an overall agreement in the LEMP shape. Consider for instance the electric field measured at 2000 m away from the flash (Figure 1a) and the electric field computed from the currents yielded by the DLCRM simulation. We note that both the initial sharp rise to peak of the electric field (because of the convex shaped portion of the current we observed) followed by a ramp like portion to it are observed in both measured and calculated portions.

Consider now the magnetic field at ground level, and 2000 m away from the lightning flash. Compare it to the measured magnetic field (Figure 1b). We note that in both cases a sub-microsecond rise to peak, followed by a hump shaped decay of the magnetic field is there. It is important to notice that the initial sharp peak observed for magnetic fields has a sub-microsecond crest-time, which in turn is much less than the rise time of the current pulse. This initial peak arises due to the fact that on the sub-microsecond scale, the rate of rise of current on the wavefront was observed to drop sharply as time progressed (Figure 5); that is on a microsecond scale the sharp rise to peak may appear as a straight jump after a slow ramp like increase. The significant part of the LRS wavefront is in reality convex in shape (Figure 5). The rise time to peak current is 4 µs, which is within the 0.22 to 4.5 µs rise time measured for subsequent strokes striking towers. Moreover, although on a microsecond timescale the DLCRM calculated LRS current pulse shows a rate of rise was about 8 kA/µs, on a sub-microsecond scale the maximum rate of rise determined is about 98 kA/µs. This high rate of rise of current is due to the convex shape of one part of the LRS wavefront, and is a very important parameter in all engineering considerations, whether they are for electromagnetic compatibility considerations, induced voltage spikes in electronic circuits and power system networks or the threat to fly-by-wire aircraft.

Our identifying the rapid rise time of electric and magnetic fields with a small section of the current wavefront, indicates the importance of the convex LRS current wavefront to obtain correct estimates of the sharp, initial peak electric and magnetic fields. The return stroke model indicates that lightning strikes to open ground may be characterized by a sharply convex wavefront on small timescales. We noted that up to 200 m or so away from the lightning channel, the electric fields are controlled by the negative electric charges along the channel. These have a sharp negative going electric field. Moreover electric fields very near (for 50 m) to the lightning channel are bipolar. For positive strokes, such bipolar fields are observed at greater distances of the order of a few kilometres. The reason for the bipolar field is that near the channel the electrostatic component of the radiated field is significant. However as the lightning channel is discharged, the intermediate ($1/r^2$) and radiation (1/r) electric field terms dominate. At 2 km above the ground, and 200 m from the flash, the general trend is for the electric field to go negative, since the 0.25 mC/m or so negative charge along the lightning channel dominates as the current magnitude drops with height. At the earth end, although the charge is about 1.2 mC/m, the current and rate of rise of current are very large. Now this gives us the clue as to why in positive discharges, one observes bipolar fields even at far distances.

In positive flashes the electric charge deposited on the leader is about 10 times higher than the electric charge deposited along the channel of negative flashes. Furthermore, the rate of rise of current for positive lightning discharges is small, an average of about 2.4 kA/µs. Thus with a smaller rate of rise of currents, which results in a smaller value for the radiation (1/r) part of the electric field, the electrostatic portion ($1/r^3$) of the LRS electric field dominates close to the lightning channel. In the future, using the DLCRM reported in this paper, we hope to report more complete, detailed simulation studies and analysis of cloud-to-ground negative and positive lightning flashes, upward ground-to-cloud flashes, intra-cloud lightning flashes, and lightning flashes attached to tall ground objects and to aircraft. It is indeed encouraging that the DLCRM appears to give very close and exact representation of the downward cloud-to-ground lightning return stroke. This enables us to calculate currents and potentials normally not accessible to measurements, as well as LEMP close to the lightning flashes and above the ground at heights of interest to aircraft and rockets (Nayak et al., 2010) systems.

Conclusions

In this paper we have presented a DLCRM for subsequent LRS and unbranched first LRS. Its development from a lumped LCR model to distributed LCR model (DLCRM) was considered to obtain the limiting conditions that must be applied when numerical computations are used to solve for the return stroke currents using the DLCRM. Verification tests that could be used to test the accuracy of the numerical solutions were presented. Considering the return stroke currents measured at ground, their measured velocity and measured radiated electric and magnetic fields, it was shown that the DLCRM, simple though in its concepts and parameter specifications, gives a very accurate representation of the subsequent and unbranched first LRS. It has also been seen that the LRS current wavefront possesses a convex shaped wavefront, and that the submicrosecond current rate of rise may be as high as 100 kA/µs, whereas the microsecond value may be an order less than this. Moreover, it was found that the

near field, electrostatic portion of the radiated electric fields gives rise to negative electric fields close to the lightning flash, gradually yielding to positive transient electric fields that resemble the LRS current waveform at distances further away from the lightning channel.

And in the far field region, the radiated fields are, as expected, determined by the current rise rates. This simple, easily programmable, fast and reliable model of the LRS, namely the DLCRM, yields a tool to investigate confidently the engineering parameters of LRS at different heights of the channel and its direct and indirect interactions with power systems, aircraft and wind turbines. It is planned that in the near future, computer simulation studies of lightning attached to grounded towers, aircraft and wind turbine will be investigated using this DLCRM of LRS reported herein.

REFERENCES

Ajayi NO (1972). Acoustic Observation of Thunder and Cloud-to-Ground Flashes, J. Geophys. Res., 77: 4586-4587.

Baba Y, Rakov VA (2005). On the mechanism of attenuation of current waves propagating along a vertical perfectly conducting wire above ground: Application to lightning. IEEE Trans. Electromagn. Compat., 47: 3: 521-532.

Baba Y, Rakov VA (2007). Electromagnetic Models of the lightning return stroke. J. Geophys. Res., 112: D04102.

Balachandran NK (1983). Acoustic and Electrical Signals from Lightning. J. Geophys. Res., 88: 3879-3884.

Berger K (1967). Novel Observations on Lightning Discharges: Results of Research on Mount San Salvatore. J. Franklin. Inst., 283: 478-525.

Berger K, Anderson RB, Kroninger H (1975). Parameters of Lightning flashes, Electra., 41: 23-37.

Berger K (1977). Earth Flash, in Lightning: Physics of Lightning, R. H. Golde Ed., Academic, pp. 119-190.

Braginskii SI (1958). Theory of the Development of a Spark Channel, Soc. Phys. JEPT (English translation). 34:1068-1074.

Bruce CER, Golde RH (1941). The Lightning Discharge. J. Inst. Electr. Eng. 88: 487-520.

Cooray V, Lundquist P (1982). On characteristics of some radiation fields from Lightning and their further origin in Positive Ground Flashes, J. Geophys. Res., 87: 11203-11214,

Cooray, V 1984). Further Characteristics of Positive radiation Fields from Lightning in Sweden, J. Geophys. Res., 89: 11807-11815.

Cooray V (1993). A model for subsequent return strokes. J. Electrostst., 30: 343-354.

Cooray V (2003). On the concepts used in return stroke models applied to engineering practice. IEEE Trans. Electromagn. Compat., 45: 1: 101- 108.

Cooray V, Theethayi N (2008). Pulse propagation along transmission lines in the presence of corona and their implications to lightning return strokes. IEEE Trans. Antenna Propag., 56: 7: 1948-1959.

da F. Mattos MA, Christopoulos C (1988). A nonlinear transmission line model of the lightning return stroke. IEEE Trans, Electromagn Compat. 30: 401-406. .

da Mattos MA, Christopoulos C (1990). A model of the lightning channel, including corona, and prediction. J. Phys., D Appl. Phys., 23: 40-46.

Deindorfer D, Uman MA (1990). An improved return stroke model with specified channel base current. J. Geophys. Res., 95: 13621-13664.

Feiux RP, Gary CH, Hutzler BP, Eyebert—Berrard AR, Hubert RA, Meesters AC, Pettroud PH, Hamelin JH, Person JM (1978). Research on Artificially triggered Lightning in France, IEEE Trans. Power Apparat. Systs., 94: 725-733.

Few AA (1981), Acoustic Radiations from Lightning, in Handbook of Atmospherics, H. Volland Ed., vol. 2, CRC Press.

Fisher RJ, Uman MA (1972).Measured Electric Field Rise Times for First and Subsequent Return Strokes. J. Geophys. Res., 77: 399-407.

Fowler RG (1982). Lightning, Applied At. Collision Phys., 5: 31-67.

Guo C, Krider EP (1982). The optical and radiation electric field signatures produced by lightning return strokes. J. Geophys., 87: 8913-8922.

Hoole PRP, Hoole SRH (1987). Computing Transient Electromagnetic Fields Radiated from Lightning. J. Appl. Phys., 61(8): 3473-3475.

Hoole PRP, Hoole SRH (1988). Guided waves along an un-magnetized lightning plasma channel. IEEE Trans. Magn. MAG-24: 3165- 3167.

Hoole PRP (1993). Modeling the Lightning Earth Flash Stroke for Studying its Effects on Engineering Systems. IEEE Trans. Magn., 29: 2: 1839-1844.

Hoole PRP, Hoole SRH (1993). Simulation of Lightning Attachment to pen Ground Tall Towers and Aircraft. IEEE Trans. On Power Delivery. 8: 2: 732-738.

Hoole SRH, Hoole PRP (1996). A Modern Short Course in Engineering Electromagnetics, Oxford University Press. 387-391, 473-474.

Idone IP, Orville RE (1985). Correlated peak intensity Light Intensity and Peak Current in Triggered Lightning Subsequent Strokes, J. Geophys Res., 90: D4: 6159-6164.

Jordon DM, Uman MA (1983). Variations in light intensity with height and time from subsequent return strokes, J. Geophys. Res., 88: 6555-6562.

Lin YT, Uman MA (1973). Electric Radiation Fields of Lightning Return Strokes in Three isolated Florida Thunderstorms, J. Geophys. Res. 78: 7911-7914.

Lin YT, Uman MA, Tiller JA, Brantley RD, Beasley WH, Krider EP, Weidman CD (1979). Characterization of Lightning return stroke electric and magnetic fields from simultaneous two- station measurements, J. Geophys. Res., 84: 6307-6314.

Uman MA, Standler RB (1980). Lightning Return Stroke Models, J. Geophys. Res., 85: 1571-1583.

Little PF (1978). Transmission Line representation of a Lightning Return Stroke, J. Phys. D: Appl. Phys., 11: 1893-1910.

Master MJ, Uman MA, Lin YT, Standler KB (1981). Calculations of Lightning Return Stroke Electric and Magnetic Fields above ground, J. Geophys. Res., 86: 12127-12132.

Moosavi SS, Moini R, Sagdeghi HH (2009). Representation of a lightning return stroke as a nonlinearly loaded thin-wire antenna. IEEE Trans, Electromagnet. Compat., 51: 3: 488-498..

Mosaddeghi A, Pavanello D, Rachidi F, Rubenstein A (2007), On the inversion of the electric field at very close range from a tower struck by lightning, J. Geophys. Res., 112: D19113.

Nayak SK, Meledash T (2010). Lightning Induced Current and Voltage on a Rocket in the Presence of Its Triling Plume. IEEE Trans. Electromagn. Compat., 52: 1: 117-127.

Orville RE, Idone VP (1982). Lightning Leader characteristics in Thunderstrom research International program (TRIP), J. of Geophys. Res., 87: 11177- 11192.

Plooster MN (1971). , Numerical Model of the Return Stroke of the Lightning Discharge, Phys. Fluids, 14: 2124-2133.

Price GH, Pierce ET (1977).The Modeling of Channel Current in the Lightning return Stroke. Radio Sci., 12: 381-388.

Rachidi F, Janischewsky WA. Hussein AM, Nucci CA, Guerrieri S, Kordi SB, Chang JS (2001). Current and electromagnetic field associated with lightning return strokes to tall towers, IEEE Trans, Electromag. Compat., 43: 3: 356-367.

Rakov VA, Uman MA (1998). Review and Evaluation of Lightning Return Stroke Models Including Some Aspects of Their Applications. IEEE Trans. Electromagn. Compat., 40: 4: 403- 426.

Rakov VA, Uman MA, Rambo KJ (2005). A review of ten years of triggered lightning experiments at Camp Blanding, Florida, Atmospheric Res., 76: 503-517.

Rakov VA, Uman MA (2003). Lightning Physics and Effects, Cambridge University Press, USA..

Schonland BF, Malan DJ, Collens H (1935). Progressive Lightning II, Soc. London Ser. A., 152: 595- 625.

Schonland BF (1956). The Lightning Discharge, Handb. Phys., 22: 576-628.

Shumpert TH, M. A. Honnell MA, Lott GK (1982). Measured Spectrum

Amplitude of Lightning Sferics in the HF, VHF and UHF Bands, IEEE Trans. Electromagn. Compat., 24: 368-372.
Spitzer L (1961). Physics of Fully Ionized gases, New York: Interscience.
Strawe DF (1979). Non-linear Modeling of Lightning Return Stroke, Proceedings of the Federal Aviation Administration/Florida Institute of Technology Workshop on Grounding and Lightning Technology. ReportFAA-RD-79.6: 9-15.
Theethayi N, Cooray V (2005). On representation of the lightning return stroke process as a current pulse along a transmission line. IEEE Trans. Power Deliv., 20: 2: 823-837.
Thotappillil A, Uman MA (1994). A lightning return stroke model with height-variable discharge content. J. Geophys. Res., 99: 22773-22780.
Tiller JA, Uman MA, Lin YT, Brantley RD, and E.P. Krider EP (1976). Electric field Statistics for Close Lightning Return Strokes near Gainesville, Florida, J. Geophys. Res., 81: 4430-4434.
Uman MA (1969). Lightning, McGraw Hil.
Uman MA, Krider KP (1982). A review of Natural Lightning: Experimental Data and Modeling, IEEE Trans. Electromagn Compat. EMC- 24: 79-112.
Uman MA (1985). Lightning return stroke electric and magnetic fields, J. Geophys. Res., 90: 6121- 6130.
Uman MA (1987). The Lightning Discharge, Academic.
von Engel A (1983). Electric Plasmas, London, Taylor and Francis.
Weidman CD, Krider EP (1980), Sub microsecond structure of the return stroke waveforms, Geophys. Res. Lett., 7: 955-958.
Weidman CD, Krider KP (1982). The Fine Structure of Lightning Return Stroke Waveforms, J. Geophys. Res., 87: 6239- 6247. (1982). Correction, J. Geophys. Res., 87: 7351.